Neurobiology of Disease 130 (2019) 104531

Contents lists available at ScienceDirect

Neurobiology of Disease

journal homepage: www.elsevier.com/locate/ynbdi

The endocannabinoid system is affected by cholesterol dyshomeostasis: Insights from a murine model of Niemann Pick type C disease

Sergio Oddi[a,b,1], Paola Caporali[c,1], Jessica Dragotto[c], Antonio Totaro[b], Marzia Maiolati[c], Lucia Scipioni[b], Clotilde Beatrice Angelucci[a], Cristina Orsini[b,c], Sonia Canterini[c], Cinzia Rapino[a], Mauro Maccarrone[b,d], Maria Teresa Fiorenza[b,c,*]

[a] Faculty of Veterinary Medicine, University of Teramo, Teramo, Italy
[b] Fondazione Santa Lucia, IRCCS, Via del Fosso di Fiorano 64, 00179, Italy
[c] Department of Psychology, Division of Neuroscience and "Daniel Bovet" Neurobiology Research Center, Sapienza University of Rome, Via dei Sardi 70, 00185 Rome, Italy
[d] Department of Medicine, Campus Bio-Medico University of Rome, Rome, Italy

ARTICLE INFO

Keywords:
Lysosomal storage disorders
Genetic mouse models
Endocannabinoid system biochemistry
Behavioral phenotyping

ABSTRACT

The dyshomeostasis of intracellular cholesterol trafficking is typical of the Niemann-Pick type C (NPC) disease, a fatal inherited lysosomal storage disorder presenting with progressive neurodegeneration and visceral organ involvement. In light of the well-established relevance of cholesterol in regulating the endocannabinoid (eCB) system expression and activity, this study was aimed at elucidating whether NPC disease-related cholesterol dyshomeostasis affects the functional status of the brain eCB system. To this end, we exploited a murine model of NPC deficiency for determining changes in the expression and activity of the major molecular components of the eCB signaling, including cannabinoid type-1 and type-2 (CB_1 and CB_2) receptors, their ligands, *N*-arachidonoylethanolamine (AEA) and 2-arachidonoylglycerol (2-AG), along with their main synthesizing/inactivating enzymes. We found a robust alteration of distinct components of the eCB system in various brain regions, including the cortex, hippocampus, striatum and cerebellum, of *Npc1*-deficient compared to *wild-type* pre-symptomatic mice. Changes of the eCB component expression and activity differ from one brain structure to another, although 2-AG and AEA are consistently found to decrease and increase in each structure, respectively. The thorough biochemical characterization of the eCB system was accompanied by a behavioral characterization of *Npc1*-deficient mice using a number of paradigms evaluating anxiety, locomotor activity, spatial learning/memory abilities, and coping response to stressful experience. Our findings provide the first description of an early and region-specific alteration of the brain eCB system in NPC and suggest that defective eCB signaling could contribute at producing and/or worsening the neurological symptoms of this disorder.

1. Introduction

Cholesterol is a critical component of cell membrane microdomains, including *caveolae* (Anderson and Jacobson, 2002) and lipid rafts (Simons and Toomre, 2000) that act as platforms for signal transduction. The presence of high-affinity cholesterol-binding motifs in G-protein coupled receptors (GPCRs) of several distinct neurotransmitters, including acetylcholine, serotonin and endocannabinoid (eCB) receptors (Di Scala et al., 2016; Fantini and Barrantes, 2009; Jafurulla et al., 2011; Oddi et al., 2011), suggests a pivotal role of cholesterol in regulating neurotransmission.

The eCB system is a lipid neuroregulatory signaling system, consisting of at least two eCB-binding receptors, the type-1 and type-2 cannabinoid receptors (CB_1 and CB_2) and their endogenous ligands, *N*-arachidonoylethanolamine (AEA) and 2-arachidonoylglycerol (2-AG), the most prominent eCBs as yet known. Distinct enzymatic activities, namely, the biosynthetic enzymes *N*-acylphosphatidylethanolamine-specific phospholipase D (NAPE-PLD) and diacylglycerol lipase-α (DAGLα), and the degradative enzymes, fatty acid amide hydrolase (FAAH) and monoacylglycerol lipase (MAGL), metabolize AEA and 2-AG, respectively (Fezza et al., 2014; Piomelli, 2003). In the brain, CB_1 receptor is the most abundant GPCR and its presence in the neocortex, hippocampus, basal ganglia, cerebellum and brainstem accounts for most of the cognitive and behavioral effects of cannabinoid drugs

* Corresponding author at: Department of Psychology, Division of Neuroscience, Sapienza University of Rome, Via dei Sardi 70, 00185 Rome, Italy.
E-mail address: mariateresa.fiorenza@uniroma1.it (M.T. Fiorenza).
[1] Equally contributing authors.

https://doi.org/10.1016/j.nbd.2019.104531
Received 5 March 2019; Received in revised form 25 June 2019; Accepted 10 July 2019
Available online 11 July 2019
0969-9961/

(Mechoulam and Parker, 2013). During the last few years, the brain eCB system — by virtue of its capability of orchestrating neuromodulatory, anti-excitotoxic, anti-inflammatory and anti-oxidative actions — has emerged as a key player in several neurodegenerative disorders, including multiple sclerosis, Parkinson's disease and Alzheimer's disease (Chiurchiù et al., 2018; Di Marzo et al., 2015).

The Niemann Pick type C disorder (NPC), a genetic rare condition due to mutations of either the *NPC1* or *NPC2* gene (Vanier, 2010), provides an excellent model system to investigate how cholesterol dyshomeostasis impinges on the functioning of the eCB system. Indeed, *NPC1* or *NPC2* genes encode two proteins that co-operatively mediate the egress of endocytosed cholesterol from the late endosomal/lysosomal (LE/Ly) compartment (Kwon et al., 2009; Deffieu & Pfeffer, 2011). The disruption of their function causes the engulfment of LE/Ly compartment with unesterified cholesterol and subsequent imbalance of endoplasmic reticulum and plasma membrane cholesterol levels, thus affecting a number of signaling mechanisms (Peake and Vance, 2010; Palladino et al., 2015; Fiorenza et al., 2013, 2018). Consistent with a well-documented relevance of membrane cholesterol in regulating eCB system expression and activity (for a review see (Dainese et al., 2010), two recent studies have highlighted a link between NPC disease-related cholesterol dyshomeostasis and impairment of this neurotransmitter system in two different animal models of this disease (Galles et al., 2018; van Rooden et al., 2018).

In the cerebellum, which is the brain area primarily affected in NPC disease at an early postnatal age (Higashi et al., 1993; Nusca et al., 2014; Caporali et al., 2016; Canterini et al., 2017), 2-AG release, triggered by depolarization of Purkinje cells (PC) dendrites, causes inhibition of GABA and glutamate release at inhibitory and excitatory synapses, respectively (Marcaggi, 2015). The first phenomenon is known as depolarization-induced suppression of inhibition (DSI), whereas the second one is known as depolarization-induced suppression of excitation (DSE). CB_1 receptor expression is very high at the terminals of basket cell interneurons forming synaptic contacts at the PC axon hillock (Ashton et al., 2004) and severe motor incoordination has been linked to abnormal activation of CB_1 receptor (Stephens, 2016).

Exploiting *Npc1*-deficient mice, the present study provides a thorough analysis of expression patterns and activities of biosynthetic and catabolic eCB system enzymes, along with that of CB receptors, in various brain structures. Significant variations of the eCB system components appear brain structure-specific, although 2-AG and AEA are consistently found to decrease and increase in each structure, respectively. The biochemical characterization of the eCB system was accompanied by a behavioral characterization of *Npc1*-deficient mice at a pre-symptomatic stage of the disease, using a number of paradigms evaluating anxiety, locomotor activity, spatial learning/memory abilities, and coping response to stressful experience. The significant difference between the performance of *Npc1*-deficient and *wild-type* age-matched mice is likely associated with changes observed in the eCB system.

2. Materials and methods

2.1. Reagents

Chemicals were of the purest analytical grade. [^{3}H] AEA was purchased from Larodan Fine Chemicals, (Malmo, Sweden). AEA was obtained from Avanti Polar Lipid (Alabaster, AL, USA). A1TG (arachidonoyl-1-thio-glycerol) was purchased from Cayman Chemical (Ann Arbor, MI, USA); 5,5′-dithiobis-2-dinitrobenzoic acid was obtained from Sigma-Aldrich (St. Louis, MO, USA). All other chemicals were purchased from Sigma-Aldrich, unless stated otherwise.

2.2. Animals

Npc1$^{nmf164/nmf164}$ mice with C57BL/6J background (hereafter named *Npc1*^{nmf164} mice) obtained from heterozygous crosses were exposed to a 12 h light-dark cycle (lights on 07:00) at the temperature of 22 ± 1 °C, receiving food and water *ad libitum*. The genotypes of pups were identified by PCR analysis of tail DNA as described (Maue et al., 2012). Behavioral performances were analyzed on a cohort of 10 *Npc1*^{nmf164} and 10 *wild-type* (*wt*) littermates, obtained from 6 litters made of at least 7 pups. Because a preliminary evaluation ruled out any gender effect on behavioral performances, male and female mice were grouped together for analyses. One week after the end of behavioral testing, the animals were sacrificed to perform expression pattern and enzymatic activity analyses.

Experimental protocols and related procedures were approved by the Italian Ministry of Public Health. All experiments were conducted according to the Italian law DL 26/2014 on the protection of animals used for scientific purpose.

2.3. Sample preparation

Brains were rapidly removed from the skull and rinsed in ice-cold 10 mM phosphate buffered saline. The cerebellum was separated from the whole brain with the use of tweezers, whereas the remaining part of the brain was sectioned into 2.0 mm coronal slices using the Mouse Brain Slicer Matrix (Ted Pella, Inc., CA, USA), isolating the striatum ant the cortex from one slice and the hippocampus from the other one. Each specimen was transferred into individual tubes, weighed, immediately frozen in dry ice and stored at −80 °C until use.

2.4. Western blotting

Equal amounts of total protein/lane (50 μg/lane), obtained as described (Maccarrone et al., 2018) from selected brain areas, including the cortex, hippocampus, striatum and cerebellum of PN75-80 old *Npc1*^{nmf164} and *wt* littermate mice, were subjected to 10% SDS-PAGE under reducing conditions. Gels were then electroblotted onto nitrocellulose filters (Whatman, Springfield Mill, UK) and immunoreacted with the following antibodies: mouse anti-actin (Sigma Aldrich, cat. no. A-5441); rabbit anti-CB_1R (1:200, Cayman Chemical; cat. no. 101500); rabbit anti-CB_2R (1:200, Cayman Chemical; cat. no. 101550); rabbit anti-DAGLα (1:200, Frontier Institute, Ishikari, Japan; cat. no. AF380-1); mouse anti-FAAH(27-Y) (1:200; Santa Cruz Biotechnology, Dallas, TX, USA; cat. no. Sc-100739) and rabbit anti-MAGL (1:500; Abcam, Cambridge, UK; cat. no. Ab24701). After incubation with the appropriate horseradish peroxidase-conjugated antibody (1:10,000; Santa Cruz Biotechnology), membranes were developed using an enhanced chemiluminescence detection system, according to the manufacturer's instructions (Luminata Crescendo Western HRP substrate, Millipore, Burlington, MA, USA). Chemiluminescence signals were detected in a C-DiGit blot scanner (LI-COR, Lincoln, NE, USA) and analyzed by Image Studio Software 4.0.21 (LI-COR). Densities of protein bands in the Western blots were measured and reported as ratios (mean ± SD) between the protein of interest and the β-actin.

2.5. Membrane isolation and specific enzyme assay

Protein extracts from selected brain areas as above were diluted in ice-cold PBS supplemented with 1 mM DTT and homogenized twice by gentle sonication on ice (Bandelin Electronic GmbH & Co., Berlin, Germany). Homogenates were centrifuged at 1000 × *g* for 10 min at 4 °C, the supernatants were collected and centrifuged at 20,000 × *g* for 30 min at 4 °C. The pellets (cell membranes) were recovered and resuspended in 50 mM Tris/HCl buffer, pH 7.5, and the protein concentration measured by Bradford assay following the manufacturer's instructions (BioRad, Hercules, CA, USA). FAAH (E.C. 3.5.1.4) activity

was assayed in homogenates incubated at pH 9.0 with 10 μM [^{3}H]AEA. The release of [^{3}H]ethanolamine catalyzed by FAAH was quantified as described (Oddi et al., 2005). To evaluate DAGLα (E.C. 3.1.1.34) and MAGL (E.C. 3.1.1.23) activity, the synthetic substrates *p*-nitrophenylbutyrate and arachidonoyl-1-thio-glycerol, respectively, were used in spectrophotometric assays, as described (Iglesias et al., 2016; Ulloa and Deutsch, 2010). Enzyme activities were expressed as pmoles of product released per minute per mg of protein.

2.6. Determination of AEA and 2-AG concentrations

For the measurement of endocannabinoid levels, brain tissues were subjected to lipid extraction with chloroform/methanol (2:1, *v*/v), in the presence of d8-AEA and d8–2-AG, as internal standards (Cayman Chemicals) (Marco et al., 2015). The organic phase was dried and then analyzed by ultra-high-performance liquid chromatography-tandem mass spectrometry (UHPLC-MS/MS), using a triple quadrupole QTRAP 4500 mass spectrometer (AB Sciex, Redwood City, CA, USA) in conjunction with a PerkinElmer LC system (PerkinElmer, Waltham, MA, USA). The levels of AEA and 2-AG were then calculated on the basis of their area ratios with the internal deuterated standard signal areas, and their amounts in pmol (or nmol, for 2-AG) were normalized per g of tissue.

2.7. Behavioral testing

The determination of behavioral performances lasted about three weeks, starting on post-natal day (PN) 55, encompassing a time window in which motor impairment is not detected, yet (Caporali et al., 2016; Maue et al., 2012). The anxiety was measured by Elevated Plus Maze (EPM), spatial learning was assessed by a Water T Maze task (WTM), memory performance was assessed by Spatial Novelty Test (SNT) and stress coping strategy was assessed by Forced Swim Test (FST). The assessment of these behavioral performances always followed the same sequential order (see Fig. 2 for time schedule).

All behavioral tests, separated by 3 to 4 days of recovery, were performed during the light phase (9:00–16:00) in a sound-attenuated experimental room. Data were collected and analyzed by a fully automated video tracking system ("Ethovision" by Noldus, The Netherlands) or manually scored (FST) blindly with regard to mouse genotype.

2.7.1. EPM

This test assesses anxiety levels in rodents based on their natural aversion to open spaces (Walf and Frye, 2007). The apparatus is a cross-shaped gray plexiglass structure with a central platform and four arms (27.5 × 5.5 cm) raised 38.5 cm above the ground. Two arms are open and two arms are closed by 15-cm-high walls. The animal is placed in the central platform and allowed to freely explore the maze for 5 min. To remove olfactory cues, the apparatus is cleaned between trials. The following EPM parameters were measured: (*i*) the total number of entries in arms as an index of activity level; (*ii*) the percentage of entries in the open arms; (*iii*) and the percentage of time spent in the open arms (entries or time in open/open + closed arms ∗ 100), as indexes of anxiety levels.

2.7.2. WTM

This task assesses spatial learning strategies in an escape-motivated submerged T-maze (Asem and Holland, 2013). The T-maze is less physical demanding than the classic Morris Water Maze, and *Npc1^{nmf164}* mice at PN60 have the essential skills required for this test (swimming and immobility on the platform). The apparatus consisted of a clear plexiglass cross maze inserted within a white circular water maze (diameter: 100 cm, height: 35 cm; arms: 40 × 5 × 30 cm). The maze was filled with water (22 ± 2 °C) and non-toxic white paint was added to ensure opacity. A moveable clear plexiglass escape platform (14 × 14 cm) was located at the end of the right or left arm submerged 2 cm from the surface of the water. The entrance to the arm opposing the start-arm was blocked with a clear Plexiglas shield; the resulting T-maze forced the mouse to turn right or left rather than swimming straight ahead. Distal visual cues were present around the maze, whereas there were no dominant cues such as light or acoustic gradients. The procedure was adapted from previous studies (Campus et al., 2015). Briefly, on each of the 3 training days, mice were placed in the start arm (South) of the maze and then allowed to swim to the escape platform for 10 consecutive trials. Mice remained on the escape platform for 10s before being transferred to a holding cage for a 30 s inter-trial interval. Each trial had a maximum duration of 60 s. First entry into the arm with the submerged platform was considered as a correct response, whereas mice were charged with errors if entered the wrong arm or left the right arm before successful escape. The probe test was performed 24 h later in a single trial (day 4), the escape platform was removed, and mice were placed in the start arm (North) of the maze; first entry into an arm was noted to attribute response (same body turn) or place (dependent on distal cues) searching strategies. Reversal learning started on day 5 to assess behavioral flexibility. During this phase the platform was located in the opposite arm compared to the acquisition phase. Percentage of correct trials provided an index of the learning performance.

2.7.3. SNT

This task relies on the innate exploratory behavior and discrimination of spatial information. The procedure and the apparatus were previously described (Orsini et al., 2004). Briefly, each mouse underwent five successive 6-min sessions separated by 3 min delay. Session 1 (S1) allowed animals to familiarize with the apparatus (open field: diameter 60 cm, height 20 cm). On S2, S3, and S4 mice explored the arena now containing four objects (A: light gray plastic cone, B: gray metal drilled rectangle, C: white plastic bottle, and D: black plastic spool) always located in the same position. In S5, objects A and C were moved: the former replaced object C and the latter was placed in a new location, so that the initial configuration was changed. Object exploration was evaluated as time (seconds) spent to contact the object with the nose. Discrimination of spatial novelty was assessed by the comparison of the difference in the exploration of the Displaced Objects between S5 and S4. Thus, row data for each category of objects were transformed in duration of contact as follows: mean time of contact with the displaced object in S5 minus mean time of contact with the same object categories in S4. General levels of exploration were evaluated as total of nose contact with all the objects in sessions 2, 3, and 4. In S1 the following motor and emotional parameters were analyzed: total distance (in cm) travelled in the arena; number of vertical rearings; percentage of distances travelled in a 10-cm peripheral annulus and in the center of the arena; time in immobility; number of defecation boluses.

2.7.4. FST

This test allows the scoring of active (swimming) or passive (immobility) behavior when rodents are forced to swim in a cylinder from which there is no escape. When re-exposed to the apparatus, animals immediately exhibit levels of immobility similar to those reached by the end of the first experience, indicating a retrieval of a long-term memory (West, 1990). The apparatus and the procedure were previously described (Colelli et al., 2010). Briefly the apparatus consisted of a glass cylinder (40 cm height, 18 cm diameter) filled with 24 ± 2 °C warm water up to 30 cm height. Mice were immerged for 10 min (training session), then removed from the cylinder, wiped and returned to their home-cages. 24 h later mice were re-exposed for 5 min to the apparatus (test session). The time spent in *immobility* (total absence of active movement) and *swimming* was scored in three 5 min temporal blocks, the first two blocks referred as the training session and the third one referring to the test session.

2.8. Statistical analysis

Data analysis was performed by using STATISTICA 8.0 (StatSoft). The data were firstly tested for normality (Wilk-Shapiro's test) and homoscedasticity (Levene's test), and then analyzed by ANOVAs followed by Bonferroni's post-hoc test. When parametric assumptions were not fully met, data transformations (angular transformation for percentages) or non-parametric analyses of variance (Mann-Whitney's *U* test) were used. Differences were considered to be significant at the $p < .05$ level.

3. Results

3.1. Biochemical characterization of the eCB system in Npc1-deficient mice

To gain insights into the alterations of cerebral eCB signaling associated to NPC disease we have performed a full biochemical characterization of expression and activity of the various components of the eCB system in relevant brain areas (*i.e.*, cerebellum, cortex, hippocampus and striatum) of *wt* and *Npc1*^{nmf164} mice.

The protein abundance of both CB_1R and CB_2R measured by Western blot was found significantly reduced in the cerebellum of *Npc1*^{nmf164} mice, but not in the other areas (Table 1).

As for the content of MAGL, the major 2-AG inactivating enzyme in the rodent brain, no significant variation in its expression and activity was observed among the examined regions, although it appeared to slightly decrease at protein level in the hippocampus (Table 1). On the contrary, the protein abundance of DAGLα, the enzyme responsible for the biosynthesis of 2-AG in the brain, appeared to decrease in all areas of *Npc1*^{nmf164} mice, except the hippocampus. In particular, the reduction was highly significant in the cerebellum (3-fold reduction, $p < .001$; Fig. 1) and a bit milder in the cortex and striatum (2-fold reduction, $p < .05$; Fig. 1) (Table 1). At the same time, the enzymatic activity of DAGLα was below detection in the cerebellum (Table 2) and 2-AG levels were significantly reduced in the cerebellum, cortex and striatum and unchanged in the hippocampus (Table 3).

With respect to FAAH, the main AEA degradative enzyme, no significant changes were observed in its protein expression levels (Table 1), while its enzymatic activity was found decreased in the cortex (1.8-fold, $p < .05$) and striatum (2.0-fold, $p < .05$). The reduced activity of FAAH observed in these regions were mirrored by increased levels of AEA in the same areas (Table 3). In the present study, we did not analyze the expression of the enzymes involved in the synthesis of AEA, as the targeted disruption of the genes of possible candidates, including NAPE-PLD and glycerophosphodiester phosphodiesterase 1 (GDE1), did not cause significant reduction in the basal brain levels of AEA (Leung et al., 2006; Simon and Cravatt, 2010), indicating that the lack of these enzymes can be compensated for by an alternate route (Maccarrone, 2017).

3.2. Behavioral assessment

To our knowledge, a behavioral characterization of cognitive and emotional functions of *Npc1*^{nmf164} mice has not been performed, while a couple of studies investigated their motor abilities. The first study reporting the identification of the novel D1005G-Npc1 mutation of *Npc1*^{nmf164} sub-line also provided a description of their motor coordination impairment (Maue et al., 2012). The second study performed by our group showed that *Npc1*^{nmf164} mouse pups acquire complex motor abilities with a significant delay compared to *wt* littermates (Caporali et al., 2016). To fill this gap, in this study we challenged pre-symptomatic *Npc1*^{nmf164} PN55 mice and *wt* littermates in a number of behavioral paradigms investigating distinct cognitive and emotional functions.

3.2.1. EPM

Number of total entries, percentage of open arm entries and percentage of time spent in the open arm were independently analyzed by one-factor ANOVAs with Genotype as between factor. *Npc1*^{nmf164} and *wt* mice showed a similar number of total entries, thus indicating that mice of both genotypes were similarly explorative and confirming that absence of motor impairment in *Npc1*^{nmf164} mice at this age. However, *Npc1*^{nmf164} mice were less anxious as they performed more entries (effect of genotype: $F_{1,18} = 5.86$, $p < .05$) and stayed longer in the open arms compared to *wt* littermates (effect of genotype: $F_{1,18} = 7.51$, $p < .05$) (Fig. 3A, B).

3.2.2. WMT

Percentage of correct trials during the training was analyzed by a mixed ANOVA for repeated measure, with Genotype as between factor and Session (3 levels: training days) as within factor. All mice learned the escape response, improving their performances as trials went by (effect of sessions, $F_{2,36} = 14.57$, $p < .0001$), but the overall performances of *wt* mice was better than that of *Npc1*^{nmf164} mice (effect of genotype, $F_{1,18} = 4.84$, $p < .05$). No interaction between genotype and sessions was found. The analysis of probe trial revealed that the majority of mice were response-learners regardless the genotype. After rotation of the maze 8 *wt* and 8 *Npc1*^{nmf164} mice made a body-turn to find the platform (response strategy), and only 2 *wt* and 2 *Npc1*^{nmf164} mice used the extra-maze cues to find the platform (place strategy). One-factor ANOVA of correct trials on the reversal learning phase (day 5) revealed that *Npc1*^{nmf164} mice made more errors compared to *wt* mice (effect of genotype, $F_{1,18} = 13.57$, $p < .01$), thus showing to be perseverative and resistant to make a new learning (Fig. 3C).

Table 1
Expression levels of eCB system components in different brain areas of *wild-type* (*wt*) and Niemann Pick C1 mice (*Npc1*) of 75 days of age.

Protein	Tissues							
	Cerebellum		Cortex		Hippocampus		Striatum	
	wt	*Npc1*	*wt*	*Npc1*	*wt*	*Npc1*	*wt*	*Npc1*
CB_1	0.54 ± 0.06	0.33 ± 0.08*	0.28 ± 0.02	0.22 ± 0.04	0.33 ± 0.09	0.35 ± 0.10	0.19 ± 0.07	0.16 ± 0.06
CB_2	0.29 ± 0.03	0.21 ± 0.03*	0.73 ± 0.21	0.51 ± 0.08	0.41 ± 0.05	0.49 ± 0.09	0.08 ± 0.02	0.08 ± 0.01
DAGLα	0.93 ± 0.07	0.26 ± 0.09***	0.67 ± 0.14	0.36 ± 0.08*	0.29 ± 0.06	0.21 ± 0.08	0.37 ± 0.04	0.22 ± 0.02**
MAGL	0.93 ± 0.02	0.57 ± 0.32	0.20 ± 0.03	0.19 ± 0.02	0.19 ± 0.04	0.08 ± 0.02*	0.35 ± 0.06	0.49 ± 0.15
FAAH	0.40 ± 0.03	0.37 ± 0.05	0.29 ± 0.07	0.25 ± 0.06	1.14 ± 0.07	0.99 ± 0.14	0.26 ± 0.12	0.23 ± 0.09

Values are expressed as chemioluminescent signals determined by densitometry and normalized to β-actin. Data are shown as mean ± SD; $n = 3$ mice per group. Significance is shown as *p* value calculated using a non paired *t*-test.

* $p < .05$ *versus* corresponding *wt*.

** $p < .01$ *versus* corresponding *wt*.

*** $p < .001$ *versus* corresponding *wt*.

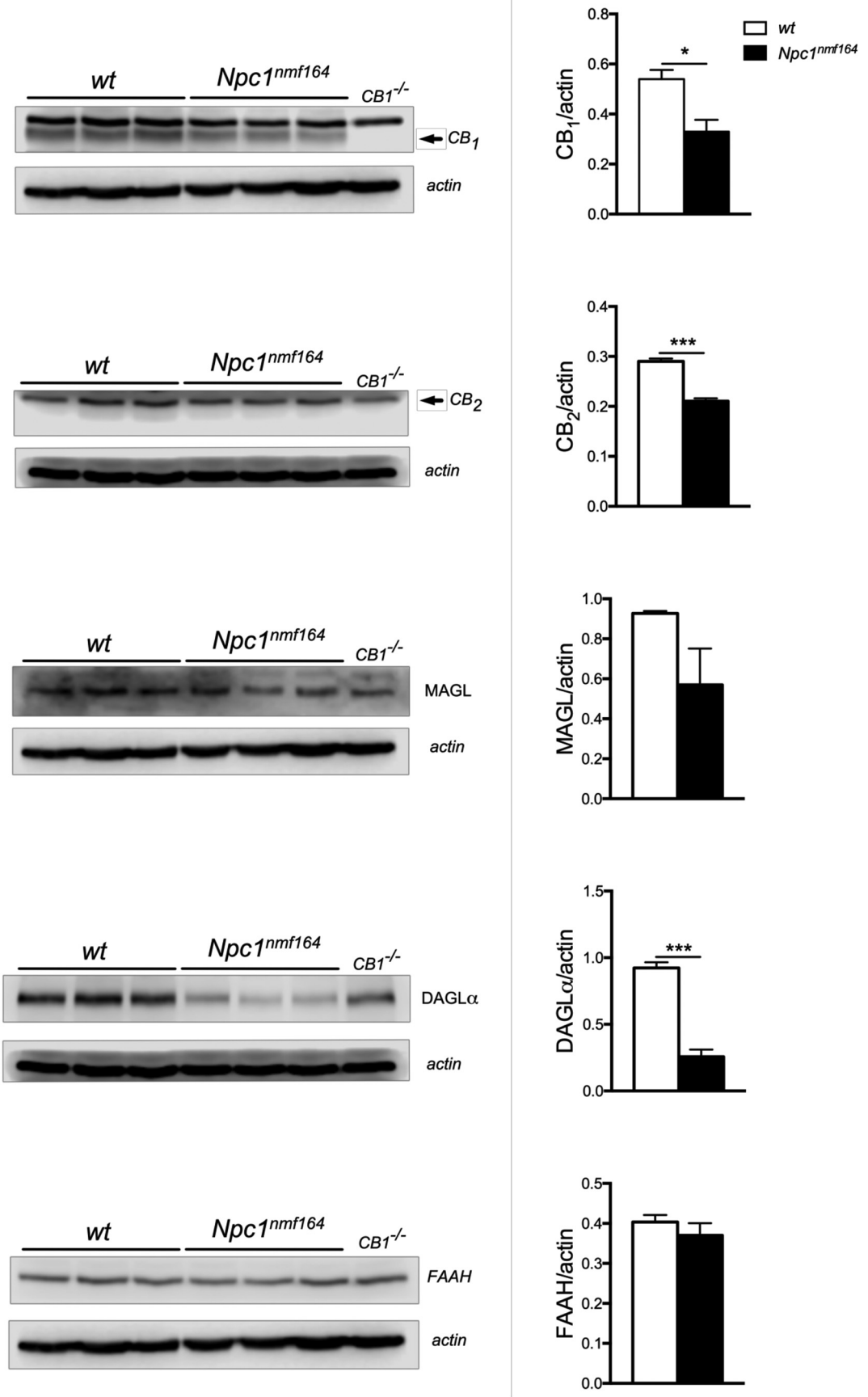

(caption on next page)

Fig. 1. Expression of different components of the eCB system in the cerebellum of *wild-type* (*wt*) and *Npc1*^{nmf164} mice. Representative immunoblots of CB_1, CB_2, MAGL, DAGLα and FAAH protein expression in the cerebellum extracts from wild-type (*wt*) and *Npc1*^{nmf164} mice of 75 days of age. Protein lysates were subjected to immunoblotting following SDS-10% PAGE against the indicated antibody. To identify the specific band for CB_1 (*arrow*), a cerebellum extract from CB_1 knock-out mice ($CB_1^{-/-}$) was also loaded. The bottom portion of the nitrocellulose membrane was probed with the anti–actin antibody, as loading control. On the right, bar graphs showing a summary of data of protein abundance. Histograms indicate the abundance (mean ± SD) of each protein determined by densitometry of protein bands obtained in at least 4 independent experiments (n = 3 mice/group) taking β-actin as internal reference. Significance is shown as p value calculated using a non paired t-test. * $p < .05$ *versus wt.* *** $p < .001$ *versus wt.*

3.2.3. SNT

Distance travelled and number of vertical rearing during familiarization with the arena (S1), were analyzed by one-factor ANOVAs. Two mice (one from each group) did not contact any objects and were excluded from statistical analyses. *Npc1*^{nmf164} mice were less active as shown by the minor distance travelled (effect of genotype: $F_{1,16} = 35.56$, $p < .0001$) and the lower number of vertical rearings (effect of genotype: $F_{1,16} = 8.20$, $p < .05$) in comparison to *wt* mice (Fig. 3D). However, no significant differences were found in time spent in immobility, thus indicating that minor distance travelled by *Npc1*^{nmf164} mice were due to slower movements. No differences were found in number of defecation boules released into the arena, suggesting no difference in their affective reaction to a novel place. However, the analysis of the arena sectors with the highest percentage of movements by the Mann-Whitney's U non-parametric test, revealed that *Npc1*^{nmf164} mice travelled less centimeters (in percentage on the total distance travelled) in the peripheral ring (effect of genotype: $U = 3.40$, $p < .001$) and more centimeters in the central arena (effect of genotype: $U = -3.58$, $p < .0001$) (Fig. 3D). This is consistent with less anxiety of *Npc1*^{nmf164} mice determined by the EPM paradigm. The time spent in object exploration in S2-S4 was analyzed by mixed ANOVA for repeated measure, with Genotype as between factor and Session (3 levels: S2, S3 and S4) as within factor. Object exploration throughout the sessions S2–S4 of the SNT was not different between the two genotypes and no habituation to the objects was developed, as time spent in contact with the objects did not decrease (Fig. 3E). Discrimination of the spatial change was evident only in *wt* mice (effect of genotype: $F_{1,16} = 5.62$, $p < .05$) as indicated by their increased exploration of the Displaced Object, while *Npc1*^{nmf164} mice failed to detect the new spatial arrangement (Fig. 3E).

3.2.4. FST

The duration of immobility and swimming was analyzed by mixed ANOVAs for repeated measure with Genotype as between factor and 5 min blocks (3 levels: block 1; block 2; test) as within factor, and results are shown in Fig. 3F. Statistical analyses of immobility revealed a significant effect of Genotype ($F_{1,18} = 193.66$, $p < .0001$) and a Genotype × time block interaction ($F_{2,36} = 11.46$, $p < .0001$). Multiple comparisons between the 5 min blocks evidenced that immobility increased in the course of the first experience only in the *wt* mice (block 1 *vs* block 2 $p < .0001$), and remained increased 24 h after the first experience (block 1 *vs* test, $p < .01$) (Fig. 3F). The analysis of swimming mirrored that of immobility, thus revealing a significant effect of Genotype ($F_{1,18} = 194.06$, $p < .0001$) and a Genotype x time block interaction ($F_{2,36} = 10.96$, $p < .0001$), and that swimming behavior decreased only in *wt* mice ($p < .0001$) and remained decreased after 24 h ($p < .01$) (Fig. 3F).

These results indicate that *Npc1*^{nmf164} mice are characterized by active coping behavior when exposed to the first experience of FST. However, while behaviors of *wt* mice expressed during the first FST experience undergo time-dependent changes, which are recalled when mice are re-exposed to the apparatus 24 h later, behaviors of *Npc1*^{nmf164} mice do not change, revealing a lack of the regular learning and recall abilities.

4. Discussion

This study provides strong evidence that the disruption of intracellular cholesterol transport associated to NPC disease markedly alters the normal state of eCB system. In particular, we found that: (*i*) the expression of CB_1 and CB_2 receptors is reduced in the cerebellum; (*ii*) the levels of 2-AG and AEA are decreased and increased, respectively, in the cerebellum and in the cerebral cortex; (*iii*) the expression and activity of 2-AG synthesizing enzyme, DAGLα, are strongly reduced in cerebellum, cortex and striatum, but not in the hippocampus; (*iv*) the activity of AEA-degrading enzyme, FAAH, is halved in cortex and striatum; and (*v*) the expression and activity of 2-AG hydrolyzing enzyme, MAGL, remain unchanged.

The finding that the eCB system in Npc1-deficient mice is affected by the dyshomeostasis of intracellular cholesterol is not surprising. Indeed, mounting evidence, largely produced by our group, indicates that the various molecular components of the eCB system are differently localized and regulated within specialized membrane subdomains, and that membrane cholesterol represents a key element in the regulation of their distribution and activity. First, we demonstrated that the CB_1 receptor physically interacts with cholesterol and upon palmitoylation it is targeted to lipid rafts (Oddi et al., 2011, 2012), as a means to down-regulate its activity (Bari et al., 2005a). By contrast, the disruption of the lipid raft microenvironment by the acute cholesterol depletion with methyl-β-cyclodextrin doubles CB_1-dependent signaling *via* adenylate cyclase and p42/p44 mitogen-activated protein kinases (Bari et al., 2005b). Second, DAGLα and 2-AG have been shown to entirely localize in lipid rafts of dorsal root ganglion cells (Rimmerman et al., 2008). Third, AEA binds cholesterol with high affinity, in a nanomolar concentration range; this interaction thereby regulates the AEA uptake, intracellular recycling and storage in adiposomes (Bari et al., 2006;

Table 2
Specific enzyme activity of FAAH, MAGL and DAGLα measured in different brain areas of *wild-type* (*wt*) and Niemann Pick C1 mice (*Npc1*) of 75 days of age.

Enzyme	Tissues							
	Cerebellum		Cortex		Hippocampus		Striatum	
	wt	*Npc1*	*wt*	*Npc1*	*wt*	*Npc1*	*wt*	*Npc1*
FAAH (pmol/min per mg)	309 ± 26	200 ± 70	640 ± 45	347 ± 70*	642 ± 50	614 ± 30	316 ± 22	155 ± 33*
MAGL (nmol/min per mg)	5.2 ± 1.1	6.4 ± 2.3	22 ± 9	24 ± 10	17 ± 3	12 ± 5	8.3 ± 3.3	14 ± 4
DAGLα (nmol/min per mg)	10 ± 2	n.d.	6.5 ± 1.4	2.5 ± 0.8*	6.4 ± 2.2	5.4 ± 2.1	3.5 ± 0.1	1.3 ± 0.8*

Data are shown as mean ± SD of values obtained in three independent determinations; n = 4–5 mice per group. Significance is shown as p value calculated using a non paired t-test. n.d.: not detectable.

* $p < .05$ *versus* corresponding *wt.*

Table 3
Levels of AEA and 2-AG measured in different brain areas of *wild-type* (*wt*) and Niemann Pick C1 mice (*Npc1*) of 75 days of age.

Endocannabinoid	Tissues							
	Cerebellum		Cortex		Hippocampus		Striatum	
	wt	*Npc1*	*wt*	*Npc1*	*wt*	*Npc1*	*wt*	*Npc1*
AEA (pmol/g)	48 ± 27	157 ± 80*	34 ± 16	57 ± 16*	20 ± 6	22 ± 9	12 ± 6	29 ± 18
2-AG (nmol/g)	5.9 ± 2.8	2.0 ± 0.72*	10.4 ± 4.2	4.9 ± 2.5*	2.3 ± 1.2	2.2 ± 1.1	9.3 ± 4.1	7.7 ± 4.5

Values are shown as mean ± SD of values obtained in three independent determinations; n = 4–5 mice per group. Significance is shown as *p* value calculated using a non paired *t*-test.

* $p < .05$ *versus* corresponding *wt*.

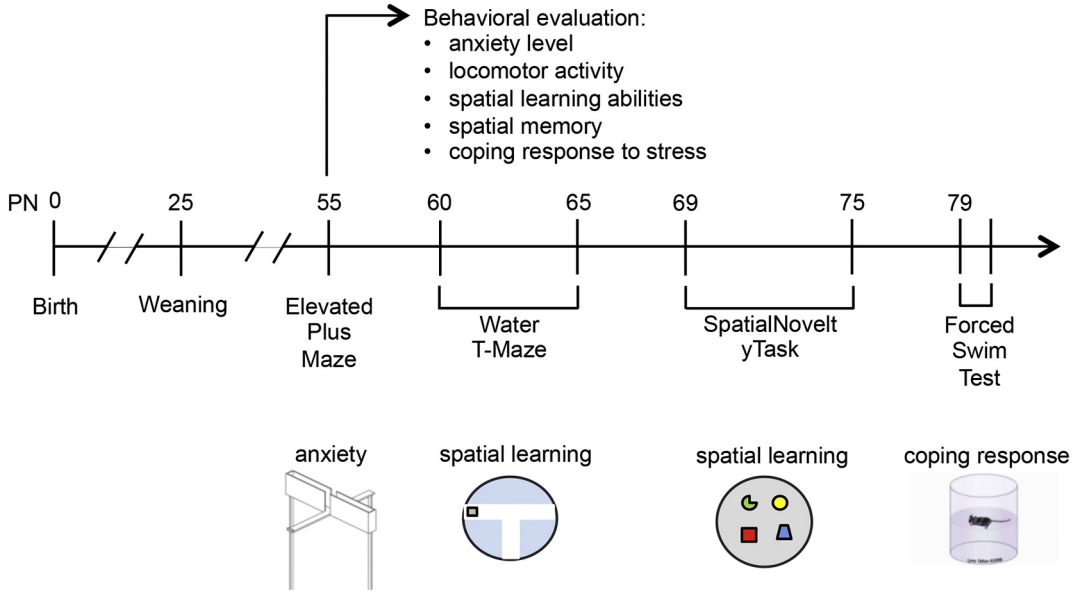

Fig. 2. A schematic summary of behavioral assessment of *wt* and age-matched *Npc1*^{nmf164} mice.

Maccarrone et al., 2010; McFarland et al., 2004; Oddi et al., 2009, 2008) influencing its overall biological effects. Finally, non-raft cholesterol modulates structure, subcellular localization and activity of FAAH (Dainese et al., 2014), while cholesterol depletion with methyl-β-cyclodextrin increases the activity of DAGLα in striatal slices (Maccarrone et al., 2009).

The findings of this study corroborate the complex role that cholesterol plays in regulating the eCB signaling, by influencing the expression, distribution and activity of distinct molecular components of the eCB system (Dainese et al., 2007, 2010). In spite of a variation of the catalytic activity, the protein level expression of FAAH did not change in Npc1-deficient mice, indicating that the regulation of this enzyme does not occur at the transcriptional level, but is based on cholesterol-dependent modification in its structure and distribution, instead (Dainese et al., 2014). On the other hand, the modulation of DAGLα expression appears to occur primarily at a translational level. In this context, it is worth noting that the impact of NPC1 deficiency on DAGLα expression and activity has been recently documented in whole brain extracts of symptomatic *Npc1*$^{nih/nih}$ (van Rooden et al., 2018).

It is very likely that the regional changes of FAAH and DAGLα, that we observed in Npc1-deficient mice, underlie the opposing changes of AEA and 2-AG. This can be appreciated in cerebellum, cortex and striatum, where the decrease of FAAH and DAGLα activity is associated to an increase of AEA and a concomitant reduction of 2-AG. These data support the notion that the two eCBs exert distinct function even in the same tissue or cell (Di Marzo, 2008). Notably, opposite changes of AEA and 2-AG have been also described for other neurodegenerative conditions, including amyotrophic lateral sclerosis, multiple sclerosis, and β-amyloid-induced neurotoxicity (Centonze et al., 2007; Di Filippo et al., 2008; Van Der Stelt et al., 2006; Witting et al., 2004).

Among the various brain structures, the cerebellum of *Npc1*^{nmf164} mice shows a significant reduction of the expression of both CB_1 and CB_2 receptors. As for the CB_1 receptor, its reduced expression likely attenuates the control on glutamate release, exacerbating the consequences of excitotoxic damage in Npc1-deficient mice were the control of extracellular glutamate is already hampered by the reduced expression of both neuronal and glial glutamate transporters (Caporali et al., 2016). On the other hand, the reduction of CB_2 receptor attenuates the defense against inflammatory events typical of the NPC disease (Baudry et al., 2003). Altogether, these findings suggest that the impairment of the eCB system may contribute at worsening the cerebellar neuropathology.

While the motor impairment of *Npc1*^{nmf164} mice has been previously characterized (Maue et al., 2012; Caporali et al., 2016), to our knowledge this is the first behavioral characterization of cognitive and emotional functions of *Npc1*^{nmf164} mice. In this study pre-symptomatic *Npc1*^{nmf164} PN55 mice and *wt* littermates were tested in a number of behavioral paradigms characterized by low motor demand, during a time window in which motor symptoms are not yet detected (see Fig. 2 for the schedule of behavioral tests). In general, the results confirmed that the motor performance of the *Npc1*^{nmf164}during the three weeks of testing was not an impediment to the behavioral performances, as evidenced by the similar number of total entries in the EPM test (Fig. 3A), and by the evidence that all mice learned the escape response in the WTM task (Fig. 3C, left), although their locomotor activity in a circular arena was slightly slower compared to *wt* mice (S1 of the SNT

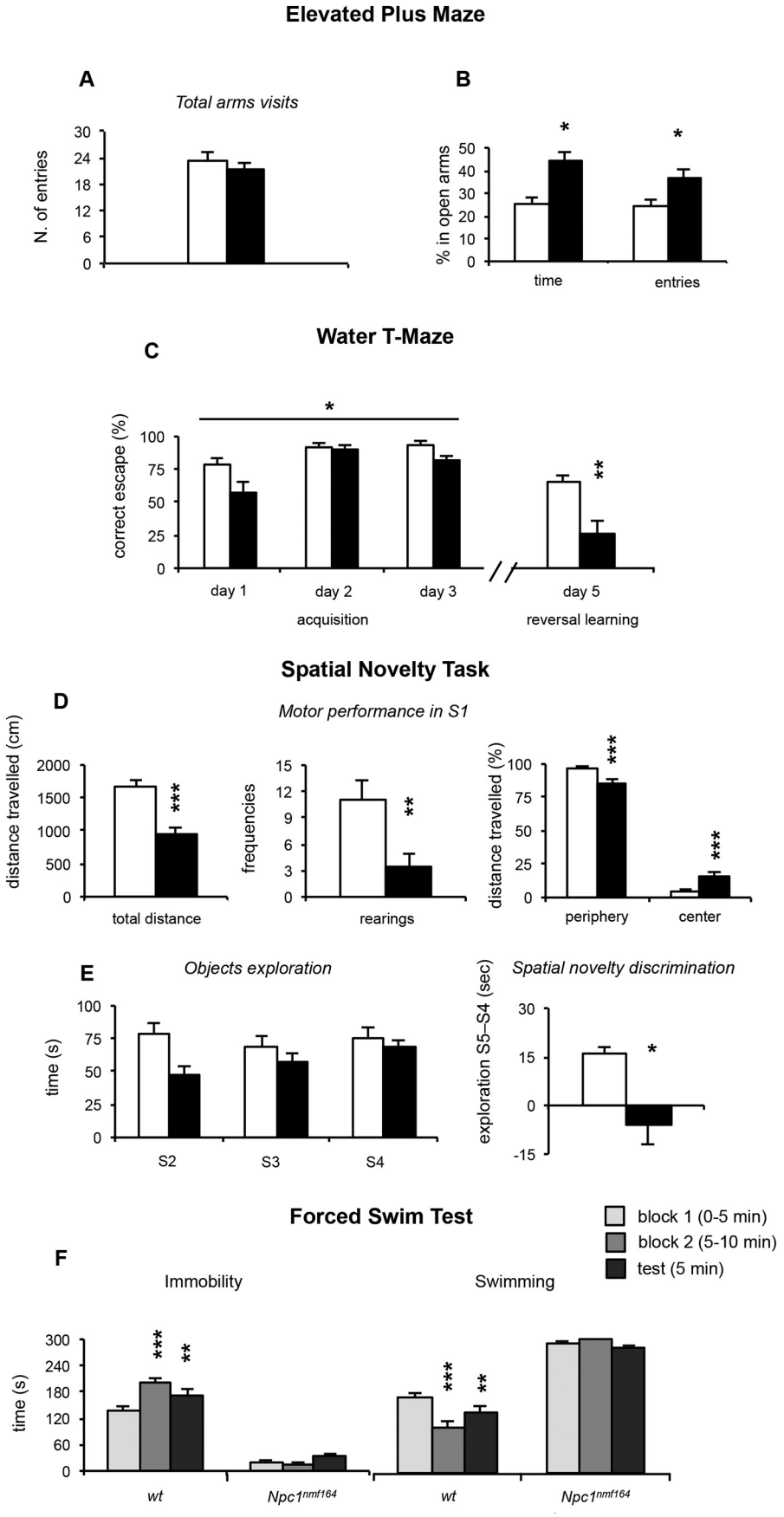

Fig. 3. Anxiety, spatial memory and stress coping response of *wt* and *Npc1*^{nmf164} mice. (A) Total visits of both arms of the elevated plus maze, and (B) time spent and number of visits in open arms. (C) Percentage of correct responses during acquisition (day 1–3) and reversal learning (day 5) of an escape response in a water T-maze. (D) Total distance travelled, number of vertical rearings and percentage of distance travelled in specific sectors, during the first session of the spatial novelty task, and (E) time spent in contact with objects during the habituation sessions and differential of time spent in contact with the displaced object between session 4 and 5. (F) Time in immobility and swimming during the first exposure to the forced swim test (blocks 1–2) and during the re-exposure 24 h later (test). Data are expressed as mean ± SEM. Empty bars: *wt* mice; full bars: *Npc1*^{nmf164} mice. $^{*}p < .05$; $^{**}p < .01$; $^{***}p < .001$.

test, Fig. 3D).

The emotional response of *Npc1*^{nmf164} mice in the EPM test revealed lower anxiety compared to the emotional reactivity of the *wt* mice (Fig. 3B), a result also confirmed by the evidence that - although slower - the *Npc1*^{nmf164} mice travelled more centimeters in the center of the open filed arena while the *wt* mice did the opposite (Fig. 3D, right). Higher exploration of the center sector of the open field is a classic measure indicating low level of anxiety, as it is normally avoided in favor of thigmotaxis behavior (Simon et al., 1994). The prevalence of swimming behaviors during the first FST experience (Fig. 3F) is indicative of an active strategy of coping with stress. Overall, these results suggest a low emotional reactivity of *Npc1*^{nmf164} mice compared to *wt* mice, however it is possible that such low reactivity may be caused by lack of the adaptive ability to recognize safety from un-safety situations, and thus be the consequence of cognitive deficits.

In the present study, cognitive performance of *Npc1*^{nmf164} mice compared to *wt* mice was dependent on the type of information to be processed in the task. Indeed, *Npc1*^{nmf164} mice were only slower learners of the escape response in the Water T-Maze task, when the escape strategy was a response-based procedural behavior (Fig. 3C, left). This task strongly favors this strategy; indeed, both *wt* and *Npc1*^{nmf164} mice first developed this strategy. However, during the reversal learning task *Npc1*^{nmf164} mice showed perseverance in the first response-based strategy, while the behavior of *wt* mice shifted toward a place-based strategy (Fig. 3C, right). Lack of flexibility in *Npc1*^{nmf164} mice might also be indicative of poor processing of spatial information. This is also in line with the compromised hippocampal-dependent memory displayed by *Npc1*^{nmf164} mice in the Spatial Novelty Discrimination task.

Increased immobility in the FST is generally considered dependent on a learning and memory process (West, 1990), that can be influenced by manipulation known to modulate memory acquisition, consolidation, and retrieval (De Pablo et al., 1989; Mitchell and Meaney, 1991), and related to learning-associated plasticity and epigenetic markers identified in brain areas of rats and mice with FST experience (Raul, 2014). Thus, lack of increased immobility in *Npc1*^{nmf164} mice is also indicative of deficits in both a learning and consolidation processes.

In conclusion, the behavioral characterization of cognitive and emotional functions of *Npc1*^{nmf164} mice - showing perseverative behavior as well as learning and memory deficits - is in line with the cognitive profile of NPC patients, as executive functions and attention have been recently found the most impaired functions together with memory impairment for some patients (Heitz et al., 2017), and learning disability were also reported (Sevin et al., 2007). Moreover, post-natal age of *Npc1*^{nmf164} mice during the behavioral testing in the present study (PN 55-80, the transition between late adolescence and emerging adulthood) matched the age of onset of cognitive impairment that has been found in NPC patients (Sevin et al., 2007).

Overall, our preclinical data document, for the first time, early and region-specific alterations in the brain eCB system, as result of NPC disease-related cholesterol dyshomeostasis, and suggest that such an impairment of the eCB signaling could contribute at generating and/or worsening neurological signs in Npc1-deficient mice. A more dedicated pharmacological study is needed to improve mechanistic understanding of the role played by the eCB system in NPC disease, and to provide evidence that targeting eCB signaling may represent a novel and effective therapeutic strategy against this devastating neurodegenerative disorder.

Acknowledgements

We are grateful to Robert P Erickson for critical reading of the manuscript. Financial support from Ministero dell'Istruzione, dell'Università e della Ricerca (under competitive PRIN 2015 grant to S.O.) and from Sapienza, grant # C26A14RMK5 to M.T.F. is gratefully acknowledged.

References

Anderson, R.G.W., Jacobson, K., 2002. A role for lipid shells in targeting proteins to caveolae, rafts, and other lipid domains. Science 296, 1821–1825. https://doi.org/10.1126/science.1068886.

Asem, J.S.A., Holland, P.C., 2013. Immediate response strategy and shift to place strategy in submerged T-maze. Behav. Neurosci. 127, 854–859. https://doi.org/10.1037/a0034686.

Ashton, J., Appleton, I., Darlington, C., Smith, P., 2004. Immunohistochemical localization of cannabinoid CB 1 receptor in inhibitory interneurons in the cerebellum. Cerebellum 3, 222–226. https://doi.org/10.1080/14734220410019011.

Bari, M., Battista, N., Fezza, F., Finazzi-Agro, A., Maccarrone, M., 2005a. Lipid rafts control signaling of type-1 cannabinoid receptors in neuronal cells. Implications for anandamide-induced apoptosis. J. Biol. Chem. 280, 12212–12220. https://doi.org/10.1074/jbc.M411642200.

Bari, M., Paradisi, A., Pasquariello, N., Maccarrone, M., 2005b. Cholesterol-dependent modulation of type 1 cannabinoid receptors in nerve cells. J. Neurosci. Res. 81, 275–283. https://doi.org/10.1002/jnr.20546.

Bari, M., Spagnuolo, P., Fezza, F., Oddi, S., Pasquariello, N., Finazzi-Agro, A., Maccarrone, M., 2006. Effect of lipid rafts on Cb2 receptor signaling and 2-arachidonoyl-glycerol metabolism in human immune cells. J. Immunol. 177, 4971–4980. https://doi.org/10.4049/jimmunol.177.8.4971.

Baudry, M., Yao, Y., Simmons, D., Liu, J., Bi, X., 2003. Postnatal development of inflammation in a murine model of Niemann-Pick type C disease: immunohistochemical observations of microglia and astroglia. Exp. Neurol. 184, 887–903. https://doi.org/10.1016/S0014-4886(03)00345-5.

Campus, P., Colelli, V., Orsini, C., Sarra, D., Cabib, S., 2015. Evidence for the involvement of extinction-associated inhibitory learning in the forced swimming test. Behav. Brain Res. 278, 348–355. https://doi.org/10.1016/j.bbr.2014.10.009.

Canterini, S., Dragotto, J., Dardis, A., Zampieri, S., De Stefano, M.E., Mangia, M.F., Erickson, R.P., Fiorenza, M.T., 2017. Shortened primary cilium length and dysregulated Sonic hedgehog signaling in Niemann-Pick C1 disease. Hum. Mol. Genet. 26, 2277–2289. https://doi.org/10.1093/hmg/ddx118.

Caporali, P., Bruno, F., Palladino, G., Dragotto, J., Petrosini, L., Mangia, F., Erickson, R.P., Canterini, S., Fiorenza, M.T., 2016. Developmental delay in motor skill acquisition in Niemann-Pick C1 mice reveals abnormal cerebellar morphogenesis. Acta Neuropathol. Commun. 4, 94. https://doi.org/10.1186/s40478-016-0370-z.

Centonze, D., Bari, M., Rossi, S., Prosperetti, C., Furlan, R., Fezza, F., De Chiara, V., Battistini, L., Bernardi, G., Bernardini, S., Martino, G., Maccarrone, M., 2007. The endocannabinoid system is dysregulated in multiple sclerosis and in experimental autoimmune encephalomyelitis. Brain 130, 2543–2553. https://doi.org/10.1093/brain/awm160.

Chiurchiù, V., van der Stelt, M., Centonze, D., Maccarrone, M., 2018. The endocannabinoid system and its therapeutic exploitation in multiple sclerosis: clues for other neuroinflammatory diseases. Prog. Neurobiol. 160, 82–100. https://doi.org/10.1016/j.pneurobio.2017.10.007.

Colelli, V., Fiorenza, M.T., Conversi, D., Orsini, C., Cabib, S., 2010. Strain-specific proportion of the two isoforms of the dopamine D2 receptor in the mouse striatum: associated neural and behavioral phenotypes. Genes Brain Behav. 9, 703–711. https://doi.org/10.1111/j.1601-183X.2010.00604.x.

Dainese, E., Oddi, S., Bari, M., Maccarrone, M., 2007. Modulation of the endocannabinoid system by lipid rafts. Curr. Med. Chem. 14, 2702–2715. https://doi.org/10.2174/092986707782023235.

Dainese, E., Oddi, S., Maccarrone, M., 2010. Interaction of endocannabinoid receptors with biological membranes. Curr. Med. Chem. 17, 1487–1499. https://doi.org/10.2174/092986710790980087.

Dainese, E., De Fabritiis, G., Sabatucci, A., Oddi, S., Angelucci, C.B., Di Pancrazio, C., Giorgino, T., Stanley, N., Del Carlo, M., Cravatt, B.F., Maccarrone, M., 2014. Membrane lipids are key modulators of the endocannabinoid-hydrolase FAAH. Biochem. J. 457, 463–472. https://doi.org/10.1042/BJ20130960.

Deffieu, M.S., Pfeffer, S.R., 2011. Niemann–Pick type C function requires luminal domain residues that mediate cholesterol-dependent NPC2 binding. Proc. Natl. Acad. Sci. USA 108, 18932–18936. https://doi.org/10.1073/pnas.1110439108.

De Pablo, J.M., Parra, A., Segovia, S., Guillamon, A., 1989. Learned immobility explains the behavior of rats in the forced swimming test. Physiol. Behav. 46, 229–237. https://doi.org/10.1016/0031-9384(89)90261-8.

Di Filippo, M., Pini, L.A., Pelliccioli, G.P., Calabresi, P., Sarchielli, P., 2008. Abnormalities in the cerebrospinal fluid levels of endocannabinoids in multiple sclerosis. J. Neurol. Neurosurg. Psychiatry 79, 1224–1229. https://doi.org/10.1136/jnnp.2007.139071.

Di Marzo, V., 2008. Targeting the endocannabinoid system: to enhance or reduce? Nat. Rev. Drug Discov. 7, 438–455. https://doi.org/10.1038/nrd2553.

Di Marzo, V., Stella, N., Zimmer, A., 2015. Endocannabinoid signalling and the deteriorating brain. Nat. Rev. Neurosci. 16, 30–42. https://doi.org/10.1038/nrn3876.

Di Scala, C., Yahi, N., Boutemeur, S., Flores, A., Rodriguez, L., Chahinian, H., Fantini, J., 2016. Common molecular mechanism of amyloid pore formation by Alzheimer's β-amyloid peptide and α-synuclein. Sci. Rep. 6, 28781. https://doi.org/10.1038/srep28781.

Fantini, J., Barrantes, F.J., 2009. Sphingolipid/cholesterol regulation of neurotransmitter receptor conformation and function. Biochim. Biophys. Acta Biomembr. 1788, 2345–2361. https://doi.org/10.1016/J.BBAMEM.2009.08.016.

Fezza, F., Bari, M., Florio, R., Talamonti, E., Feole, M., Maccarrone, M., 2014. Endocannabinoids, related compounds and their metabolic routes. Molecules 19, 17078–17106. https://doi.org/10.3390/molecules191117078.

Fiorenza, M.T., Dardis, A., Canterini, S., Erickson, R.P., 2013. Cholesterol metabolism-associated molecules in late onset Alzheimer's disease. J. Biol. Regul. Homeost.

Agents 27 (2 Suppl), 23–35.
Fiorenza, M.T., Moro, E., Erickson, R.P., 2018. The pathogenesis of lysosomal storage disorders: beyond the engorgement of lysosomes to abnormal development and neuroinflammation. Hum. Mol. Genet. 27 (R2), R119–R129. https://doi.org/10.1093/hmg/ddy155.
Galles, C., Prez, G.M., Penkov, S., Boland, S., Porta, E.O.J., Altabe, S.G., Labadie, G.R., Schmidt, U., Knölker, H.-J., Kurzchalia, T.V., de Mendoza, D., 2018. Endocannabinoids in Caenorhabditis elegans are essential for the mobilization of cholesterol from internal reserves. Sci. Rep. 8, 6398. https://doi.org/10.1038/s41598-018-24925-8.
Heitz, C., Epelbaum, S., Nadjar, Y., 2017. Cognitive impairment profile in adult patients with Niemann pick type C disease. Orphanet J. Rare Dis. 12, 166. https://doi.org/10.1186/s13023-017-0714-1.
Higashi, A., Murayama, S., Pentchev, P.G., Suzuki, K., 1993. Cerebellar degeneration in the Niemann–Pick type C mouse. Acta Neuropathol. 85, 175–184. https://doi.org/10.1007/BF00227765.
Iglesias, J., Lamontagne, J., Erb, H., Gezzar, S., Zhao, S., Joly, E., Truong, V.L., Skorey, K., Crane, S., Madiraju, S.R.M., Prentki, M., 2016. Simplified assays of lipolysis enzymes for drug discovery and specificity assessment of known inhibitors. J. Lipid Res. 57, 131–141. https://doi.org/10.1194/jlr.D058438.
Jafurulla, M., Tiwari, S., Chattopadhyay, A., 2011. Identification of cholesterol recognition amino acid consensus (CRAC) motif in G-protein coupled receptors. Biochem. Biophys. Res. Commun. 404, 569–573. https://doi.org/10.1016/J.BBRC.2010.12.031.
Kwon, H.J., Abi-Mosleh, L., Wang, M.L., Deisenhofer, J., Goldstein, J.L., Brown, M.S., Infante, R.E., 2009. Structure of N-terminal domain of NPC1 reveals distinct subdomains for binding and transfer of cholesterol. Cell 137, 1213–1224.
Leung, D., Saghatelian, A., Gabriel, M., Simon, A., Cravatt, B.F., 2006. Inactivation of N-acyl phosphatidylethanolamine phospholipase D reveals multiple mechanisms for the biosynthesis of endocannabinoids. Biochemistry 45, 4720–4726. https://doi.org/10.1021/BI060163L.
Maccarrone, M., 2017. Metabolism of the endocannabinoid anandamide: open questions after 25 years. Front. Mol. Neurosci. 10, 166. https://doi.org/10.3389/fnmol.2017.00166.
Maccarrone, M., De Chiara, V., Gasperi, V., Viscomi, M.T., Rossi, S., Oddi, S., Molinari, M., Musella, A., Finazzi-Agrò, A., Centonze, D., 2009. Lipid rafts regulate 2-arachidonoylglycerol metabolism and physiological activity in the striatum. J. Neurochem. 109, 371–381. https://doi.org/10.1111/j.1471-4159.2009.05948.x.
Maccarrone, M., Dainese, E., Oddi, S., 2010. Intracellular trafficking of anandamide: new concepts for signaling. Trends Biochem. Sci. 35, 601–608. https://doi.org/10.1016/j.tibs.2010.05.008.
Maccarrone, M., Totaro, A., Leuti, A., Giacovazzo, G., Scipioni, L., Mango, D., Coccurello, R., Nisticò, R., Oddi, S., 2018. Early alteration of distribution and activity of hippocampal type-1 cannabinoid receptor in Alzheimer's disease-like mice overexpressing the human mutant amyloid precursor protein. Pharmacol. Res. 130, 366–373. https://doi.org/10.1016/j.phrs.2018.02.009.
Marcaggi, P., 2015. Cerebellar endocannabinoids: retrograde signaling from purkinje cells. Cerebellum 14, 341–353. https://doi.org/10.1007/s12311-014-0629-5.
Marco, E.M., Rapino, C., Caprioli, A., Borsini, F., Laviola, G., Maccarrone, M., 2015. Potential therapeutic value of a novel FAAH inhibitor for the treatment of anxiety. PLoS One 10, e0137034. https://doi.org/10.1371/journal.pone.0137034.
Maue, R.A., Burgess, R.W., Wang, B., Wooley, C.M., Seburn, K.L., Vanier, M.T., Rogers, M.A., Chang, C.C., Chang, T.-Y., Harris, B.T., Graber, D.J., Penatti, C.A.A., Porter, D.M., Szwergold, B.S., Henderson, L.P., Totenhagen, J.W., Trouard, T.P., Borbon, I.A., Erickson, R.P., 2012. A novel mouse model of Niemann-Pick type C disease carrying a D1005G-Npc1 mutation comparable to commonly observed human mutations. Hum. Mol. Genet. 21, 730–750. https://doi.org/10.1093/hmg/ddr505.
McFarland, M.J., Porter, A.C., Rakhshan, F.R., Rawat, D.S., Gibbs, R.A., Barker, E.L., 2004. A role for caveolae/lipid rafts in the uptake and recycling of the endogenous cannabinoid anandamide. J. Biol. Chem. 279, 41991–41997. https://doi.org/10.1074/jbc.M407250200.
Mechoulam, R., Parker, L., 2013. The endocannabinoid system and the brain. Annu. Rev. Psychol. 64, 21–47. https://doi.org/10.1146/annurev-psych-113011-143739.
Mitchell, J.B., Meaney, M.J., 1991. Effects of corticosterone on response consolidation and retrieval in the forced swim test. Behav. Neurosci. 105, 798–803. https://doi.org/10.1037/0735-7044.105.6.798.
Nusca, S., Canterini, S., Palladino, G., Bruno, F., Mangia, F., Erickson, R.P., Fiorenza, M.T., 2014. A marked paucity of granule cells in the developing cerebellum of the Npc1(−/−) mouse is corrected by a single injection of hydroxypropyl-beta-cyclodextrin. Neurobiol. Dis. 70, 117–126. https://doi.org/10.1016/j.nbd.2014.06.012.
Oddi, S., Bari, M., Battista, N., Barsacchi, D., Cozzani, I., Maccarrone, M., 2005. Confocal microscopy and biochemical analysis reveal spatial and functional separation between anandamide uptake and hydrolysis in human keratinocytes. Cell. Mol. Life Sci. 62, 386–395. https://doi.org/10.1007/s00018-004-4446-8.
Oddi, S., Fezza, F., Pasquariello, N., De Simone, C., Rapino, C., Dainese, E., Finazzi-Agro, A., Maccarrone, M., 2008. Evidence for the intracellular accumulation of anandamide in adiposomes. Cell. Mol. Life Sci. 65, 840–850. https://doi.org/10.1007/s00018-008-7494-7.
Oddi, S., Fezza, F., Pasquariello, N., D'Agostino, A., Catanzaro, G., De Simone, C., Rapino, C., Finazzi-Agrò, A., Maccarrone, M., Finazzi-Agro, A., Maccarrone, M., 2009. Molecular identification of albumin and Hsp70 as cytosolic anandamide-binding proteins. Chem. Biol. 16, 624–632. https://doi.org/10.1016/j.chembiol.2009.05.004.
Oddi, S., Dainese, E., Fezza, F., Lanuti, M., Barcaroli, D., De Laurenzi, V., Centonze, D., Maccarrone, M., 2011. Functional characterization of putative cholesterol binding sequence (CRAC) in human type-1 cannabinoid receptor. J. Neurochem. 116, 858–865. https://doi.org/10.1111/j.1471-4159.2010.07041.x.
Oddi, S., Dainese, E., Sandiford, S., Fezza, F., Lanuti, M., Chiurchiu, V., Totaro, A., Catanzaro, G., Barcaroli, D., De Laurenzi, V., Centonze, D., Mukhopadhyay, S., Selent, J., Howlett, A.C., Maccarrone, M., 2012. Effects of palmitoylation of Cys(415) in helix 8 of the CB(1) cannabinoid receptor on membrane localization and signalling. Br. J. Pharmacol. 165, 2635–2651. https://doi.org/10.1111/j.1476-5381.2011.01658.x.
Orsini, C., Buchini, F., Conversi, D., Cabib, S., 2004. Selective improvement of strain-dependent performances of cognitive tasks by food restriction. Neurobiol. Learn. Mem. 81, 96–99. https://doi.org/10.1016/S1074-7427(03)00075-3.
Palladino, G., Loizzo, S., Fortuna, A., Canterini, S., Palombi, F., Erickson, R.P., Mangia, F., Fiorenza, M.T., 2015. Visual evoked potentials of Niemann-Pick type C1 mice reveal an impairment of the visual pathway that is rescued by 2-hydroxypropyl-ß-cyclodextrin. Orphanet. J. Rare. Dis. 10, 133. https://doi.org/10.1186/s13023-015-0348-0.
Peake, K.B., Vance, J.E., 2010. Defective cholesterol trafficking in Niemann-Pick C-deficient cells. FEBS Lett. 584, 2731–2739.
Piomelli, D., 2003. The molecular logic of endocannabinoid signalling. Nat. Rev. Neurosci. 4, 873–884. https://doi.org/10.1038/nrn1247.
Raul, J.M., 2014. Making memories of stessful events: a journey along epigenetic, gene transcription, and signaling pathways. Front. Psychiatry 5, 5. https://doi.org/10.3389/fpsyt.2014.00005.
Rimmerman, N., Hughes, H.V., Bradshaw, H.B., Pazos, M.X., Mackie, K., Prieto, A.L., Walker, J.M., 2008. Compartmentalization of endocannabinoids into lipid rafts in a dorsal root ganglion cell line. Br. J. Pharmacol. 153, 380–389. https://doi.org/10.1038/sj.bjp.0707561.
Sevin, M., Lesca, G., Baumann, N., Millat, G., Lyon-Caen, O., Vanier, M.T., Sedel, F., 2007. The adult form of Niemann-Pick disease type C. Brain 130, 120–133. https://doi.org/10.1093/brain/awl260.
Simon, P., Depuis, R., Costentin, J., 1994. Thigmotaxis as an index of anxiety in mice. Influence of dopaminergic transmissions. Behav. Brain Res. 61 (1), 59–64.
Simon, G.M., Cravatt, B.F., 2010. Characterization of mice lacking candidate N-acyl ethanolamine biosynthetic enzymes provides evidence for multiple pathways that contribute to endocannabinoid production in vivo. Mol. BioSyst. 6, 1411. https://doi.org/10.1039/c000237b.
Simons, K., Toomre, D., 2000. Lipid rafts and signal transduction. Nat. Rev. Mol. Cell Biol. 1, 31–39. https://doi.org/10.1038/35036052.
Stephens, G.J., 2016. Does modulation of the endocannabinoid system have potential therapeutic utility in cerebellar ataxia? J. Physiol. 594, 4631–4641. https://doi.org/10.1113/JP271106.
Ulloa, N.M., Deutsch, D.G., 2010. Assessment of a spectrophotometric assay for monoacylglycerol lipase activity. AAPS J. 12, 197–201. https://doi.org/10.1208/s12248-010-9180-6.
Vanier, M.T., 2010. Niemann-Pick disease type C. Orphanet J. Rare Dis. 5, 16–33. https://doi.org/10.1186/1750-1172-5-16.
Van Der Stelt, M., Mazzola, C., Esposito, G., Matias, I., Petrosino, S., De Filippis, D., Micale, V., Steardo, L., Drago, F., Iuvone, T., Di Marzo, V., 2006. Endocannabinoids and β-amyloid-induced neurotoxicity in vivo: effect of pharmacological elevation of endocannabinoid levels. Cell. Mol. Life Sci. 63, 1410–1424. https://doi.org/10.1007/s00018-006-6037-3.
Van Rooden, E.J., van Esbroeck, A.C.M., Baggelaar, M.P., Deng, H., Florea, B.I., Marques, A.R.A., Ottenhoff, R., Boot, R.G., Overkleeft, H.S., Aerts, J.M.F.G., van der Stelt, M., 2018. Chemical proteomic analysis of serine hydrolase activity in Niemann-Pick type C mouse brain. Front. Neurosci. 12, 440. https://doi.org/10.3389/fnins.2018.00440.
Walf, A.A., Frye, C.A., 2007. The use of the elevated plus maze as an assay of anxiety-related behavior in rodents. Nat. Protoc. 2 (2), 322–328.
West, A.P., 1990. Neurobehavioral studies of forced swimming: the role of learning and memory in the forced swim test. Prog. Neuro-Psychopharmacol. Biol. Psychiatry 14, 863–877. https://doi.org/10.1016/0278-5846(90)90073-P.
Witting, A., Weydt, P., Hong, S., Kliot, M., Moller, T., Stella, N., 2004. Endocannabinoids accumulate in spinal cord of SOD1G93Atransgenic mice. J. Neurochem. 89, 1555–1557. https://doi.org/10.1111/j.1471-4159.2004.02544.x.